Available online at www.sciencedirect.com
SCIENCE DIRECT®
Journal of Power Sources 145 (2005) 139–146
JOURNAL OF POWER SOURCES
www.elsevier.com/locate/jpowsour

Preparation and application of nanoporous carbon templated by silica particle for use as a catalyst support for direct methanol fuel cell

Pil Kim, Heesoo Kim, Ji Bong Joo, Wooyoung Kim, In Kyu Song, Jongheop Yi *

School of Chemical Engineering, Institute of Chemical Processes, Seoul National University, Shinlim-dong, Kwanak-ku, Seoul 151-744, Republic of Korea

Accepted 3 January 2005
Available online 20 April 2005

Abstract

Polymer-silica composites were synthesized by resorcinol–formaldehyde polymerization in the presence of uniform size silica particles. After carbonization and subsequent removal of the silica template, these polymer-silica composites turned into nanoporous carbon xerogel with high surface area and large pore size. By controlling the initial pH of the carbon precursor solution, nanoporous carbons with different textural properties could be fabricated. As the pH of the reaction mixture was decreased, the pore size of nanoporous carbon increased because the aggregated silica particles, i.e., larger templates, were generated in low pH condition. Although the pore size of nanoporous carbon was increased with decreasing pH, the templating effect was reduced with decreasing pH, leading to the formation of significant microporous carbon framework in carbon xerogels. For DMFC application, the PtRu (1:1) alloy was supported on nanoporous carbons and activated carbon by a formaldehyde reduction method. It was revealed that the textural properties of carbon supports played important roles in the metal dispersion and DMFC performance of the supported PtRu catalysts. The support with large pore size and high surface area (especially, meso-macropore area) was favorable for high dispersion of PtRu catalyst and easy formation of triple-phase boundary. Microporous framework, resulted from the destruction of structural integrity, was insufficient for high dispersion of PtRu species. The catalysts with higher metal dispersion and structural integrity showed higher catalytic activities in the methanol electro-oxidation and the DMFC performance test.

Keywords: Nanoporous carbon; Templating method; Direct methanol fuel cell; PtRu catalyst

1. Introduction

Porous carbon materials have been extensively investigated in many fields of science and technology due to their pronounced textural properties and an inert nature in an extreme pH condition [1–4]. High surface area and large pore volume made them suitable for an adsorbent of a pollutant [2] and a substrate of catalytically active metal [4]. Typical examples of these porous carbons are aerogel and xerogel carbons that made from polymerizable hydrocarbons such as resorcinol and formaldehye [5,6]. Although the carbon aerogel has exhibited better textural properties such as relatively large pore size with high surface area and large pore volume than the carbon xerogel, the preparation procedures are much more complicated. In other words, carbon xerogel can be more easily prepared and has an economic advantage, although its textural properties are inferior to those of carbon aerogel, since a drastic surface tension can be induced between vapor–liquid interfaces during the drying of polymeric compound carbonized, resulting in the collapse of the pore structure [7]. Recently, the templating method has been successfully applied for the preparation of porous materials such as silica [8], alumina [9] and carbon xerogel [10–12]. In particular, the carbon xerogels prepared by this method were found to have excellent textural properties such as high surface area and large pore volume, often together with regular pore size. There have been many studies for the preparation and application of nanoporous carbon xerogel fabricated by a templating route [10–14]. It was reported that a nanoporous

* Corresponding author. Tel.: +82 2 880 7438; fax: +82 2 888 7295.
E-mail address: jyi@snu.ac.kr (J. Yi).

0378-7753/$ – see front matter © 2005 Elsevier B.V. All rights reserved.
doi:10.1016/j.jpowsour.2005.01.070

carbon could be prepared using colloidal silica as a template and the resulting carbon material exhibited higher adsorption capacity for bulky dyes than the commercial activated carbon [13]. It was also reported that the highly ordered nanoporous silica could be templated into a nanoporous carbon with an excellent nanoporosity, leading to an enhanced electrochemical property [15]. The excellent pore properties such as high surface area with large pore size allowed these kinds of material to be a good support for catalysts for use in the polymer electrolyte fuel cell, where carbon supported Pt-based catalysts with high metal loadings are required for the desirable power density. For example, Joo et al. [16] prepared a nanoporous carbon by an ordered silica templating method and tested as a catalyst support for a fuel cell. They [16] pointed out that the ordered pore structure with high surface area were favorable for high dispersion of Pt particles, which led to an excellent catalytic activity of Pt-nanoporous carbon catalyst. Another report [14] demonstrated that a porous carbon, which was fabricated using silica particles as a porogen, could serve as a support for a finely dispersed catalyst with high metal contents, leading to an excellent catalytic performance in direct methanol fuel cell (DMFC) [14].

In this work, nanoporous carbon xerogels were prepared by sol–gel polymerization of resorcinol and formaldehyde in the presence of silica particles and subsequent carbonization, followed by selective etching of silica particle. Pore properties of the prepared carbon materials were extensively investigated with a variation of pH of the initial precursor solution. The prepared carbons were finally used as a support for PtRu alloy catalyst for DMFC, and the effects of pore properties on the DMFC performance were examined.

2. Experimental

2.1. Preparation of carbon supports and supported catalysts

Nanoporous carbon xerogels (NCs) were synthesized using colloidal silica particles (Ludox HS 40 with an average particle size of 12 nm, Aldrich) as a template by polymerization of resorcinol (Junsei) and formaldehyde (35 wt.% aqueous solution, Aldrich) as a carbon precursor, followed by subsequent carbonization and removal of silica particles. Na_2CO_3 (Aldrich) was used as a polymerization catalyst for carbon precursor and the molar ratio of the catalyst to resorcinol was fixed at 1:50. In a typical synthesis, an aqueous mixture containing resorcinol and formaldehyde (molar ratio of 1:2) was added to the silica colloidal solution. The pH of the reaction mixtures was adjusted with 1 N HNO_3 or NH_4OH (35 wt.% aqueous solution, Aldrich) to obtain mixtures with pH values of 1.5, 5 and 9. The reaction mixtures were sealed in a closed vessel and stirred vigorously with Na_2CO_3 solution for 2 h at room temperature, until viscous slurries with a color of light brown were obtained. The slurries were cured at 85 °C for 72 h, and resultant resorcinol–formaldehyde gels containing silica particles (R–F-silica composite) were cooled to room temperature. Nanoporous carbon xerogels (NCs) were finally obtained by the pyrolysis of R–F-silica composite at 800 °C, followed by the selective etching of silica components. The prepared NC was denoted as NC-pH value. For example, NC-5 represents the NC prepared from a reaction mixture with pH value of 5.

Prepared NCs were used as a support for PtRu alloy catalysts. The PtRu-NCs (60 wt.% metal loading with 1:1 alloy ratio) were prepared by a modified formaldehyde reduction method reported in a literature [17]. In a typical procedure, NC was suspended in an appropriate amount of deionized water and then metal precursors ($H_2PtCl_6{\cdot}xH_2O$ and $RuCl_3{\cdot}xH_2O$, Fluka) were added. After the pH of the reaction mixture was adjusted to be 12 using 1 M NaOH solution, excess amounts of formaldehyde were added to reduce metal ions with vigorous magnetic stirring. The reaction mixture was heated up to 90 °C and kept at this temperature for 5 h. $NaNO_3$ was slowly added into the solution in order for the sedimentation of metal nanoparticles on the carbon support. The resultant black precipitate was washed with large amounts of water, and it was then dried at 120 °C for overnight.

2.2. Characterization

Crystalline phases of the prepared catalysts were identified by X-ray diffraction with Cu Kα radiation (XRD, M18XHF-SRA, MAC/Science). Nitrogen adsorption–desorption isotherms were obtained with an ASAP-2010 (Micromeritics) apparatus. The pore size distribution was determined by the BJH method applied to the adsorption branch of the N_2 isotherm. Pore sizes and morphologies of the prepared samples were investigated by transmission electron microscopy (TEM, Joel, JXA-8900R) and field emission scanning electron microscopy (FE-SEM, JSM-6700F).

The cyclic voltammograms were obtained using a conventional three-electrode system with saturated calomel and platinum gauge as a reference and a counter electrode, respectively. The reference electrode was prepared by coating a small amount of catalyst ink on disk-type graphite. Prior to coating with catalyst ink, the graphite surface was polished by alumina paste and washed with de-ionized water. Cyclic voltammograms were obtained at room temperature at a scan rate of 20 mV s^{-1} in 0.5 M H_2SO_4 solution containing 1 M CH_3OH (EG & G 263A Potentiostat).

2.3. MEA preparation and single cell test

The membrane electrode assembles (MEAs) were fabricated according to the method described in literatures [18,19]. Both sides of electrode were composed of a carbon paper and a carbon-supported catalyst layer. The anode contained the prepared PtRu-NCs with a metal loading of 3 mg cm^{-2}, and the cathode contained the commercial 40 wt.% Pt/C cata-

lyst (Johnson Matthey) with a metal loading of 4 mg cm^{-2}. Nafion-117 membrane was used as solid electrolyte, which was pretreated by boiling with 3 wt.% H_2O_2 for 3 h and then in 0.5 M H_2SO_4 solution. The anode-membrane-cathode was assembled by hot-pressing at 120 °C for 2 min. Two molar of methanol solution was fed to the single cell with an effective area of 5 cm^2. The fuel cell system was operated at 75 °C, and the methanol feed rate was controlled to be 1.0 ml min^{-1} using masterflex pump (Cole-Parmer Instrument Co.). On the cathode side, dry oxygen was fed at a rate of 500 ml min^{-1}.

3. Results and discussion

3.1. Textual properties of supports and supported catalysts

N_2 adsorption–desorption isotherms and pore size distributions (PSDs) of NCs are shown in Figs. 1 and 2, respectively. All the NCs exhibited a sharp capillary condensation at high relative pressure, which could not found in the isotherm of activated carbon (AC). The NC-9 showed the type IV isotherm with H2 hysteresis loop that is a typical characteristic feature of mesoporous materials, while NC-1.5 exhibited type II isotherm indicating the existence of pores larger than 50 nm. The N_2 adsorption–desorption isotherm of NC-5 showed an intermediate feature between NC-1.5 and NC-5. These results were well supported by the pore size distribution of NCs, as shown in Fig. 2. Relatively narrow peak

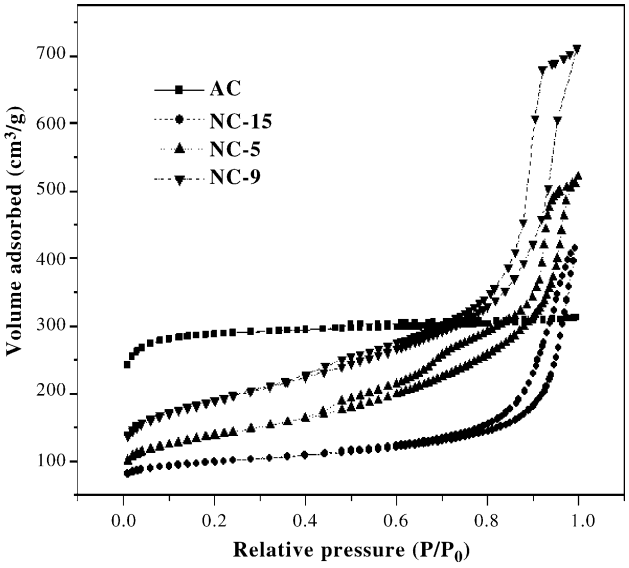

Fig. 1. N_2 adsorption–desorption isotherms of carbon supports.

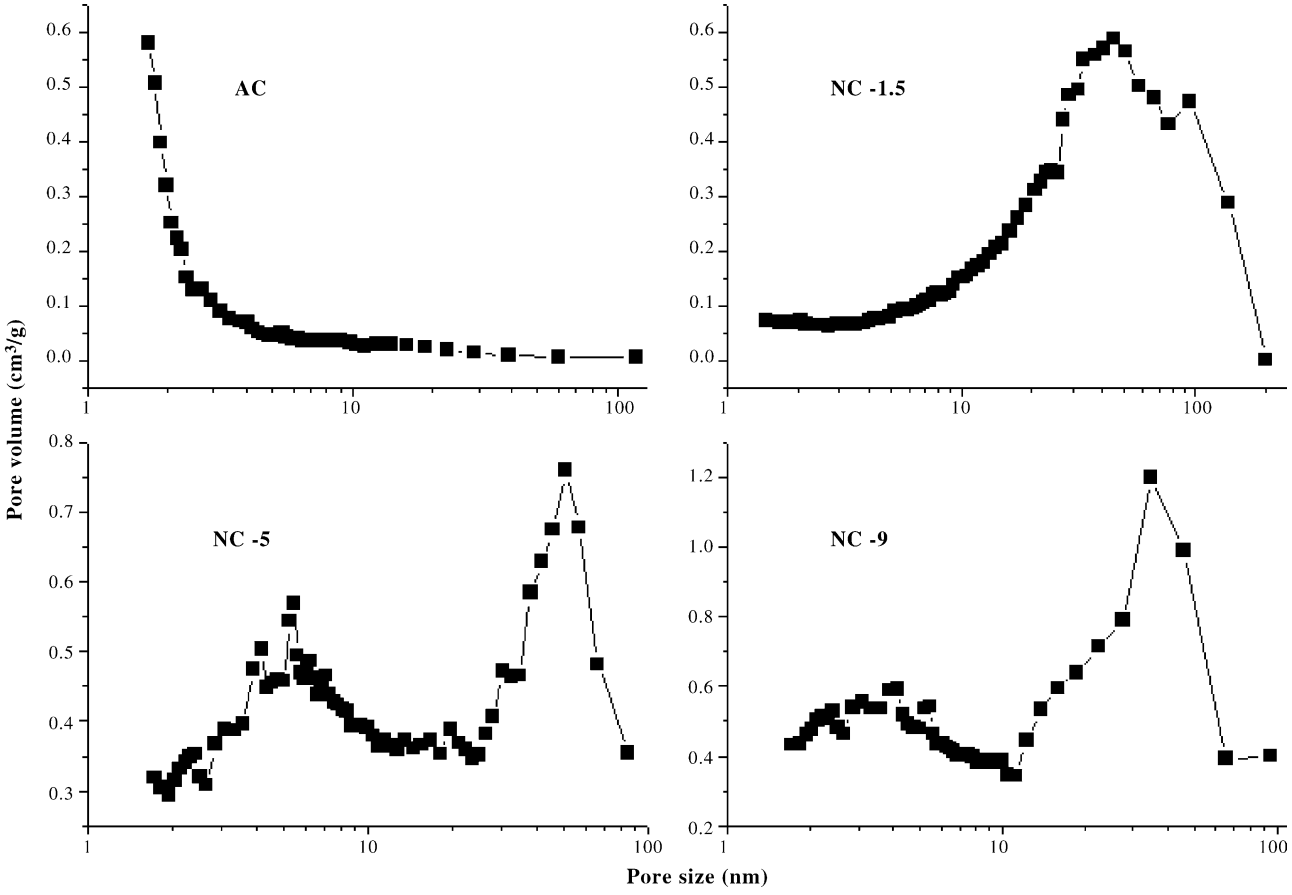

Fig. 2. Pore size distributions of carbon supports.

of PSD appeared at ca. 40 nm and ca. 50 nm for NC-9 and NC-5, respectively. On the other hand, NC-1.5 showed broad bimodal PSD center at around 50 and 90 nm. Silica colloidal particles used in this work as a pore generator have an average particle size of ca. 12 nm. Therefore, large pore size observed for NC-1.5 and NC-5 samples is unusual. When the initial pH of colloidal silica solution is high as in the case of NC-9, silica colloids are stabilized at this pH value. However, the stability of silica sol decreases with increasing the acidity of the solution, and subsequently, the aggregation of silica sol can occur [13,20]. Therefore, large pores of NC-1.5 and NC-5 may be understood in a manner that silica sols are aggregated one another with decreasing pH value of synthesis mixture, which leads to large size of template, and in the long run, large pore size. In addition, judging from the pore size of NC-9, the aggregation of silica particles would be unavoidable even in which the condition of the silica particles are stabilized.

Textural properties of supports and supported catalysts are summarized in Table 1. BET surface area and micropore area of AC are highest, and the ratio of meso-macropore area with respect to micropore area is lowest among support materials. The BET surface area of NCs also reflects both meso-macropores and micropores, indicating the generation of micropores was inevitable during the pyrolysis of R–F polymer in the preparation of NC support [14,21]. The contribution of micropore area to total surface area (BET surface area) became significant as the pH of initial reaction mixture decreased. It is likely that the polymer framework without template effect is generated with decreasing pH of reaction mixture due to the formation of the large size silica template. Since the micropores are originated from the polymer structure carbonized that eventually will be carbon framework, the higher portion of micropore in NC-1.5 can be attributed to the lower degree of silica templating effect.

Fig. 3 shows the N_2 adsorption–desorption isotherms of supported PtRu catalysts. Compared to the isotherms shown in Fig. 1, N_2 isotherm of a supported catalyst is very similar to that of the corresponding support, indicating that basic pore structures of the supports are not altered upon metal loading.

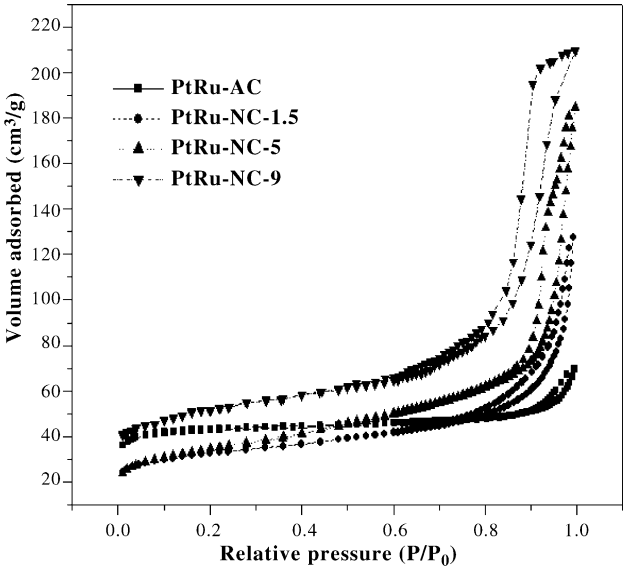

Fig. 3. N_2 adsorption–desorption isotherms of supported PtRu catalysts.

Fig. 4 shows the pore size distributions (PSD) of supported catalysts. Compared to the PSDs shown in Fig. 2, the PtRu-NC catalysts exhibited slightly decreased pore sizes due to loading of the nanosize metal particle on the pore surface [14]. As listed in Table 1, surface area and pore volume of the supports were significantly decreased after the supporting of metals. In particular, the contribution of micropore to the textural properties became drastically decreased in the supported catalysts, demonstrating that the micropores were blocked by or covered with metal species.

3.2. Morphological observation of pore structure and pore size

Fig. 5 shows the TEM images of NC supports. All the NC supports were found to have spherical pores. The trend of pore size was well consistent with the result of N_2 isotherms; the largest pore size was observed for NC-1.5 and the smallest for NC-9. These features of pore structure and size could

Table 1
Textural properties of supports and supported catalysts

	S_{BET}[a] ($m^2\ g^{-1}$)	S_{micro}[b] ($m^2\ g^{-1}$)	$S_{meso\text{-}macro}$[c] ($m^2\ g^{-1}$)	$S_{meso\text{-}macro}/S_{micro}$	V_{micro}[d] ($cm^3\ g^{-1}$)	V_{total}[e] ($cm^3\ g^{-1}$)
AC	901	759	142	0.187	0.38	0.48
NC-1.5	321	202	119	0.589	0.10	0.56
NC-5	467	164	303	1.84	0.081	0.77
NC-9	654	217	437	2.01	0.11	1.10
PtRu-AC	346	253	93	0.36	0.084	0.13
PtRu-NC-1.5	94	57	37	0.65	0.018	0.11
PtRu-NC-5	133	55	78	1.42	0.018	0.18
PtRu-NC-9	145	67	78	1.16	0.02	0.22

[a] BET surface area.
[b] Micropore surface area.
[c] Meso-macropore surface area.
[d] Micropore volume.
[e] Total pore volume.

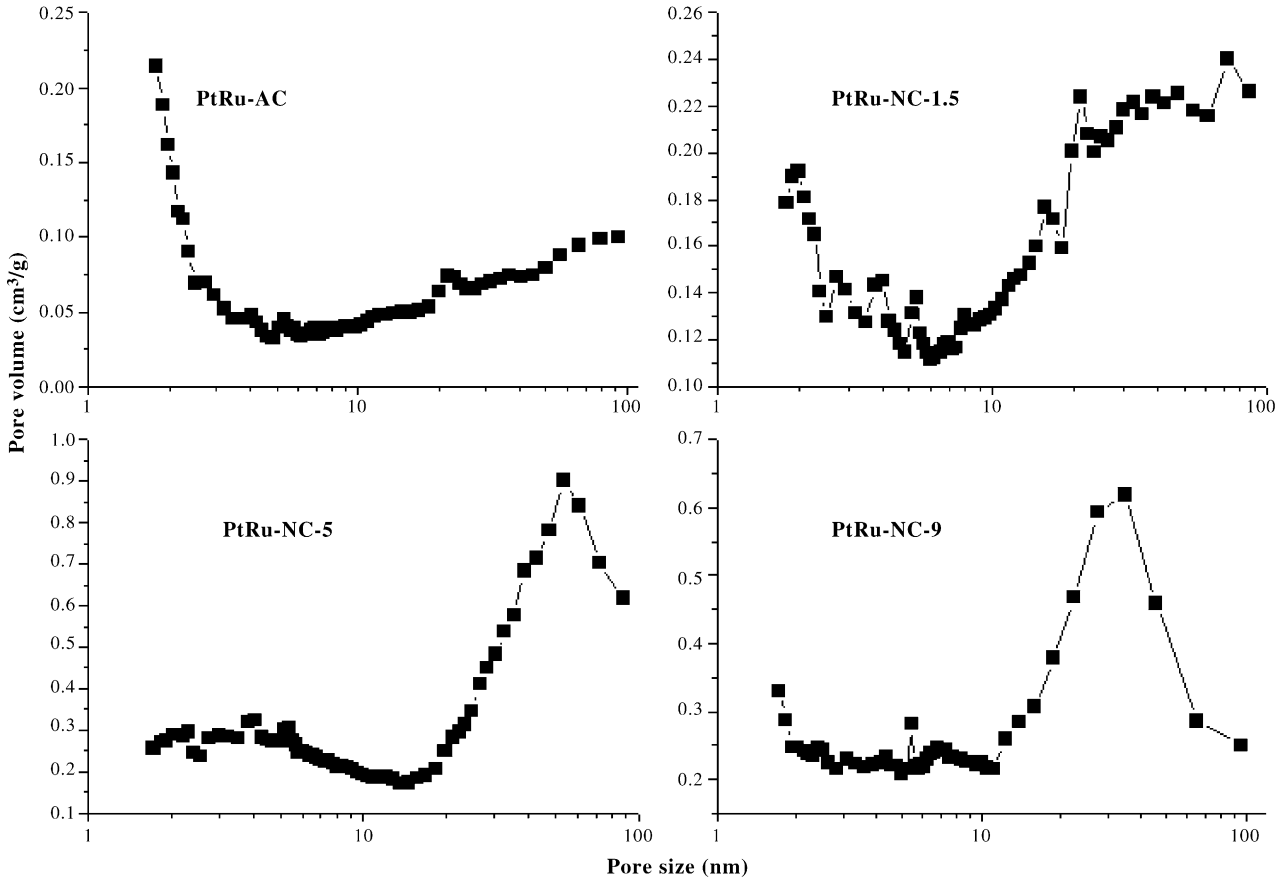

Fig. 4. Pore size distributions of supported PtRu catalysts.

also be elucidated by FE-SEM images, as shown in Fig. 6. It is noticeable that NC-1.5 shows both large size pores and large portion of non-porous framework. Compared to the other two NC supports, the NC-1.5 exhibited high degree of micropore area, generated from the polymer structure that was non-templated by silica particle. Therefore, it is likely that the non-porous framework observed for NC-1.5 is essentially microporous, because FE-SEM is not enough to resolve micropores of the NC-1.5. However, only a small part of non-templated framework was observed in the NC-5. These results are well consistent with N_2 adsorption–desoroption experimental results.

3.3. Alloy phase and metal particle size

Fig. 7 shows the XRD patterns of NC-5 support and supported catalysts. As shown in Fig. 7(a), two characteristic XRD peaks were observed at 23° and 43° in the NC-5 support, suggesting that NC-5 support is not completely amorphous and contains a part of crystalline phase [21]. Both NC-1.5 and NC-9 supports exhibited the same XRD pattern as NC-5.

XRD patterns of the supported alloy catalysts are shown in Fig. 7(b). It is noticeable that no diffraction peaks related to pure Ru or Ru-rich hexagonal close packed (hcp) phase were observed. In particular, the characteristic peaks for pure Pt (1 1 1) and (2 2 0) appearing at 39.76° and 67.45°, respectively, were shifted to the higher angle, for example, 40.30° and 68.41°, respectively, for PtRu-AC. These results indicate that the face-centered cubic (fcc) structure of PtRu alloy is dominant on the supported catalyst [22].

Average metal particle size of prepared catalysts was calculated according to the Debye–Scherrer equation as listed in Table 2. The alloy metals on NC-5 and NC-9 are smaller than those of on AC and NC-1.5. It has been generally accepted that physicochemical properties of the supported metal catalysts are affected by many factors such as preparation conditions, metal loadings, and physical–chemical properties of support (pore structure and surface properties) [23]. When

Table 2
Average particle size calculated from the (2 2 0) position using the Debye–Scherrer equation[a]

	D_{XRD} (nm)
PtRu-AC	3.1
PtRu-NC-1.5	2.8
PtRu-NC-5	2.4
PtRu-NC-9	2.2

[a] $D = (0.94\lambda)/(B\cos\theta_B)$, where D is average particle size, λ is X-ray wavelength, θ_B is (2 2 0) peak position, and B represents the FWMH value of radian scale.

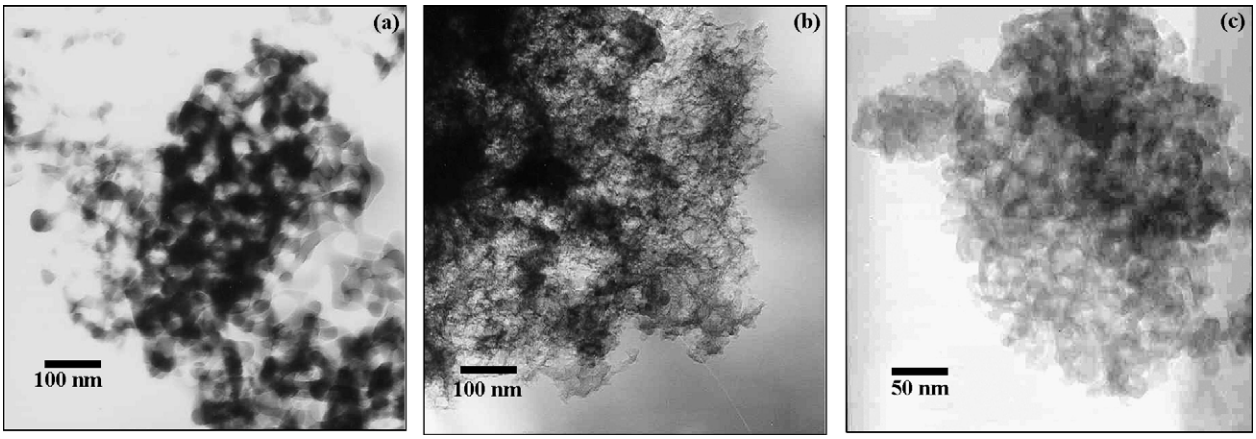

Fig. 5. TEM images of carbon supports: (a) NC-1.5, (b) NC-5 and (c) NC-9.

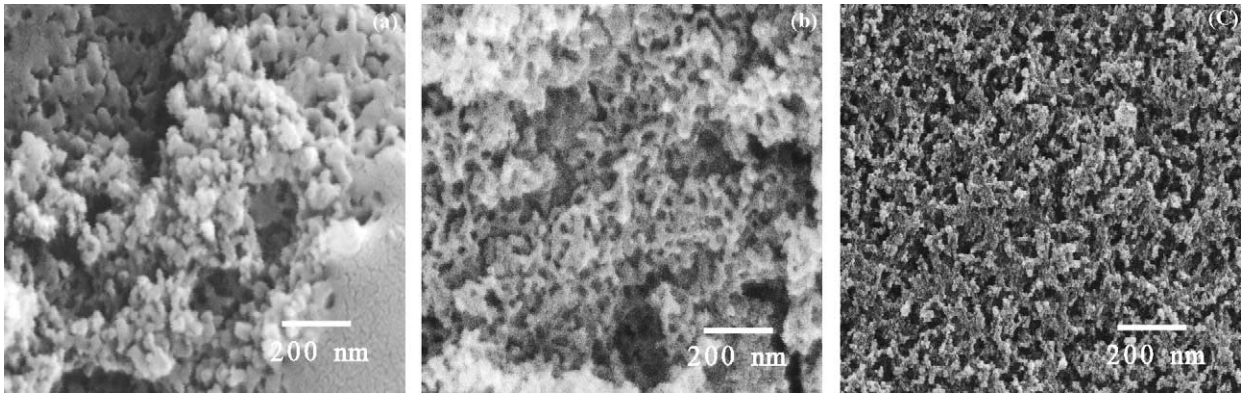

Fig. 6. FE-SEM images of nanoporous carbons prepared by silica particle templating method: (a) NC-1.5, (b) NC-5 and (c) NC-9.

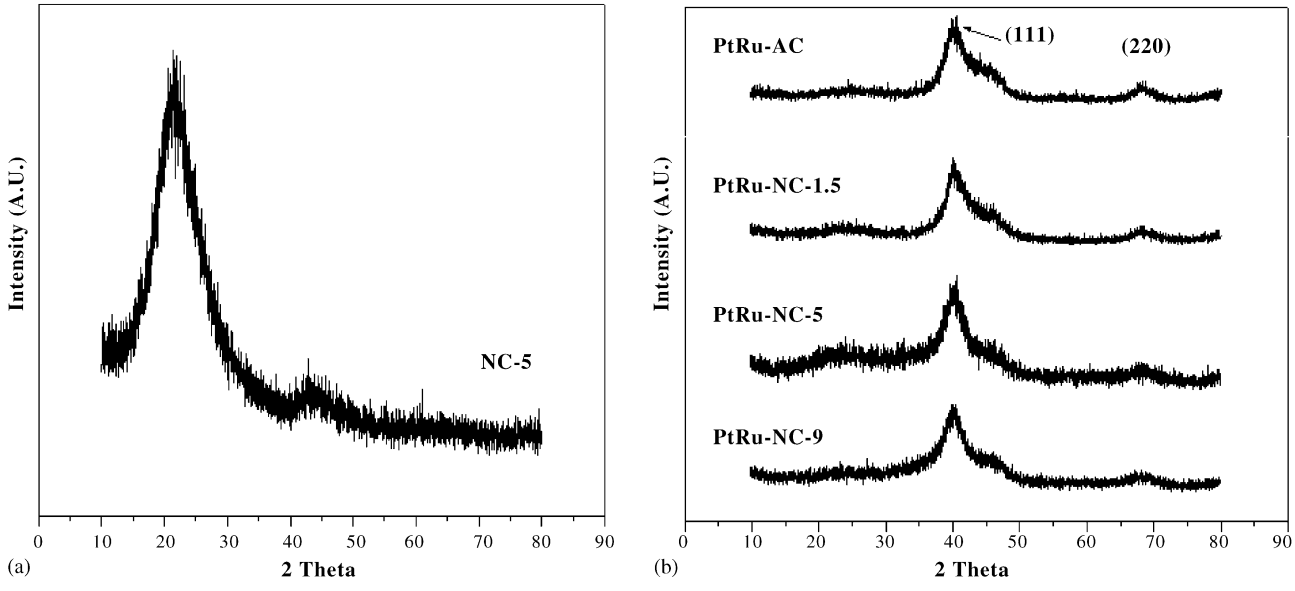

Fig. 7. XRD patterns of NC-5 and NC-supported PtRu catalysts.

considering that the same preparation method and metal loading were imposed in all the catalysts in this study, it is expected that other factors affect in the formation of different size metal particles on carbon support. In principle, it is believed that both pore structure and surface properties of supports may affect in the formation of different size metal particles. Surface properties of NC supports are expected to be almost identical, since R–F polymers produced from the same precursor were carbonized in the same conditions. Despite of the same surface properties, however, it was observed that PtRu-NC-1.5 showed larger metal particle size than the other two NC-supported catalysts. In addition, the some portion of mesopores of NC-5 and NC-9 disappeared after metal loadings (Fig. 2, Fig. 4, and Table 1), indicating the pore blocking by metal particles. Although this may cause a drastic decrease of surface area and pore volume, the metal aggregation could be prevented by the role of small pores as a barrier. Joo et al. [16] reported the preparation and application of porous carbon with high surface area and uniform pore size. They [16] observed that small and uniform pores of porous carbon could serve as an individual nanoscale reactor or a barrier for metal aggregation, and were very effective for the formation of finely dispersed metal particles with high level of metal contents. In our supported catalyst system, the micropores of carbon support did not effectively act as a barrier, and consequently, the metal aggregation was prominent in the catalysts supported on AC and NC-1.5 (these supports exhibited high portion of micropore area). Additionally, it was found that the catalysts supported on NC-9, which showed the highest value of meso-macropore area, had the smallest metal particle size among the catalysts.

3.4. Catalytic performance in half and single cell

Fig. 8 shows the cyclic voltammograms of supported catalysts for methanol electro-oxidation. The methanol electro-oxidation begins at about 0.25 V versus SCE for all the catalysts tested in this work, which is typical for PtRu catalyst in the methanol electro-oxidation [24,25]. In addition, the values of maximum current density at 0.5 V were different from one another, and decreased in the order PtRu-NC-9 ≥ PtRu-NC-5 > PtRu-NC-1.5 ≥ PtRu-AC. What is interesting is that the activity trend is the same as metal dispersion trend. The supported metal catalysts on a reactive support such as alumina and titania retain their unique metal-support interaction, which are considered as a critical factor for the catalytic activity [26,27]. On the other hand, carbons are known to be an inert support, and therefore, the interaction between metal and carbon would be very weak. It can be concluded, therefore, that the metal dispersion on the carbon support rather than metal–carbon interaction is a decisive factor determining the catalytic activity in the methanol electro-oxidation in this research.

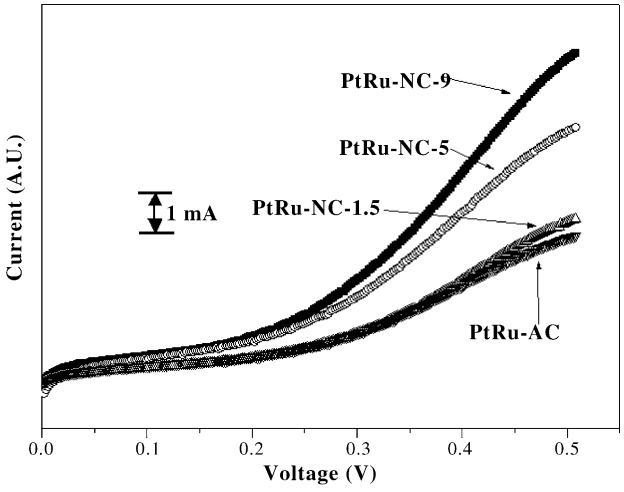

Fig. 8. Voltammograms of supported alloy catalysts for methanol electro-oxidation in 0.5 M H_2SO_4 + 2 M CH_3OH with a scan rate of 20 mV s^{-1}.

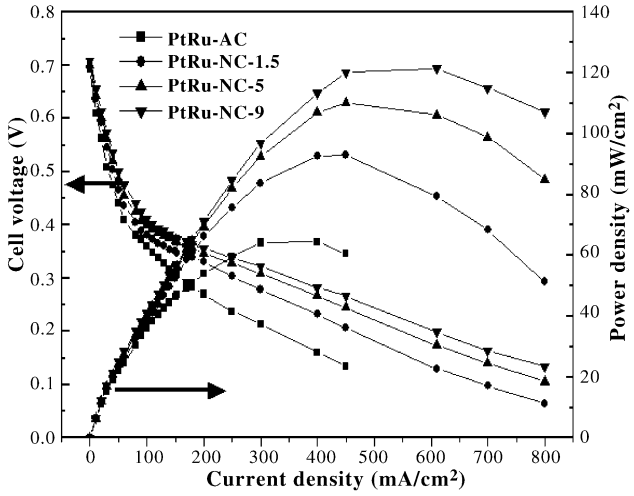

Fig. 9. DMFC single cell performance of supported catalysts at 75 °C.

Fig. 9 shows the single cell performance of supported catalysts for direct methanol fuel cell (DMFC) at 75 °C. The open circuit voltages (OCVs) were 0.694, 0.697, 0.701, and 0.709 V for PtRu-AC, PtRu-NC-1.5, PtRu-5, and PtRu-9, respectively. The maximum power densities were 64.5, 93.1, 110.3, and 121.4 for PtRu-AC, PtRu-NC-1.5, PtRu-5, and PtRu-9, respectively. Since one kind of catalyst with the same metal loading was coated on the cathode side, the variations of OCV and maximum power density values can be totally attributed to the performance of anode catalysts, meaning the catalytic activity in the methanol electro-oxidation. In this work, the trend for cell performance was similar to that for methanol electro-oxidation activity. It is inferred that the different dispersion of active metal particles was responsible for the variation in the catalytic activity of methanol electro-oxidation. In addition to the metal dispersion, the pore size and the structural integrity of supporting materials played an important role in the single cell performance.

According to a literature [14], the structural integrity of a support is important for the catalytic activity. In this research, the structural integrity might be destroyed as the size of template increased, which spontaneously resulted in the formation of non-templating framework. The electro-chemical catalysis in fuel cell takes place in the interface between catalyst surface and electrolyte, i.e., triple-phase boundary [28]. Contrary to cyclicvoltammetry experiments using liquid electrolyte, a solid electrolyte (or an ionomer) of large size is employed in a single cell test. Therefore, a support with high surface area and large pore size is favorable for both metal dispersion and ionomer diffusion. In this viewpoint, it is likely that the micropores of AC are not efficient in the metal dispersion as well as in the formation of triple-phase boundary. Therefore, it can be concluded that higher activities of PtRu-NC-5 and PtRu-NC-9 are attributed to the favorable pore structure, which leads to high metal dispersion and easy formation of triple-phase boundary.

4. Conclusions

Nanoporous carbon xerogels were fabricated by the sol–gel polymerization of resorcinol and formaldehyde in the presence of uniform size silica particles as a template and subsequent carbonization, followed by selective removal of the silica template. Nanoporous carbons with different pore structures could be prepared by controlling the initial pH of the synthesis mixture. As the pH was decreased, the pore size of nanoporous carbon was significantly increased and the templating effect was suppressed, leading to the formation of a greater portion of microporous carbon framework in the resulting carbon xerogels. In this work, nanoporous carbons and commercial activated carbon were used for the support of PtRu catalyst for direct methanol fuel cell. It was revealed that the textural property of carbon supports played important roles in the metal dispersion and DMFC performance of the supported PtRu catalysts. The support with large pore size and high surface area, especially in the meso-macropore area, was favorable for the dispersion of PtRu metal species and for the formation of triple-phase interface. It was believed that the microporous framework, resulting from the destruction of structural integrity, was not efficient for high dispersion of PtRu catalyst. High catalytic activity and DMFC performance of PtRu-NC-5 and PtRu-NC-9 were attributed to the favorable pore properties of the corresponding carbon supports, such as high meso-macropore area with large pore size and structural integrity, which resulted in high dispersion of metal species and easy formation of triple-phase boundary.

Acknowledgement

This work was supported by National Research Laboratory (NRL) program of the Korea Science and Engineering Foundation (KOSEF).

References

[1] S. Sircar, T.C. Golden, M.B. Rao, Carbon 34 (1996) 1–12.
[2] V.B. Fenelonov, V.A. Likholobov, A.Y. Derevyankin, M.S. Mel'gunov, Catal. Today 42 (1998) 341–345.
[3] B.S. Girgis, A.-N.A. El-herdawy, Micro. Meso. Mater. 52 (2002) 105–117.
[4] Y.X. Wang, S.H. Tan, D.L. Jiang, X.Y. Zhang, Carbon 41 (2003) 2065–2072.
[5] R.W. Pekala, J. Mater. Sci. 24 (1989) 3221–3227.
[6] X. Lu, M.C. Arduini-Schuster, J. Kuhn, O. Nilsson, J. Fricke, R.W. Pekala, Science 225 (1992) 971–974.
[7] S.A. Al-Muhtaseb, J.A. Ritter, Adv. Mater. 15 (2003) 101–114.
[8] W.W. Lukens Jr., G.D. Stucky, Chem. Mater. 14 (2002) 1665–1670.
[9] Y. Kim, C. Kim, J. Yi, Mater. Res. Bul. 39 (2004) 2103–2112.
[10] R. Ryoo, S.H. Joo, S. Jun, J. Phys. Chem. B 103 (1999) 7743–7746.
[11] J. Lee, K. Sohn, T. Hyeon, J. Am. Chem. Soc. 123 (2001) 5146–5147.
[12] J.-S. Yu, S. Kang, S.B. Yoon, G. Chai, J. Am. Chem. Soc. 124 (2002) 9382–9383.
[13] S. Han, K. Sohn, T. Hyeon, Chem. Mater. 12 (2000) 3337–3341.
[14] G.S. Chai, S.B. Yoon, J.-S. Yu, J.-H. Choi, Y.-E. Sung, J. Phys. Chem. B 108 (2004) 7074–7079.
[15] J. Lee, S. Yoon, S.M. Oh, C.-H. Shin, T. Hyeon, Adv. Mater. 12 (2000) 359–362.
[16] S.H. Joo, S.J. Choi, I. Oh, J. Kwak, Z. Liu, O. Terasaki, R. Ryoo, Nature 412 (2001) 169–172.
[17] Z. Zhou, W. Zhou, S. Wang, G. Wang, L. Jiang, H. Li, G. Sun, Q. Xin, Catal. Today 93 (2004) 523–528.
[18] Z.B. Wei, S.L. Wang, J.G. Liu, J. Power Source 93 (2004) 364–369.
[19] Y. Wang, J. Ren, K. Deng, L. Gui, Y. Tang, Chem. Mater. 12 (2000) 1622–1627.
[20] C.J. Brinker, G.W. Scherer, Sol–Gel Science, Academic Press, San Diego, 1990, pp. 97–297.
[21] C. Lin, J.A. Ritter, Carbon 35 (1997) 1271–1278.
[22] S.-A. Lee, K.-W. Park, J.-H. Choi, B.-K. Kwon, Y.-E. Sung, J. Electr. Soc. 149 (2002) A1299–A1304.
[23] G. Ertl, H. Knozinger, J. Weitkamp (Eds.), Handbook of Heterogeneous Catalysis, vol. 1, VCH, Weinheim, Federal Republic of Germany, 1997, pp. 191–283.
[24] G.T. Burstein, C.J. Barnett, A.R. Kucernak, K.R. Williams, Catal. Today 38 (1997) 425–437.
[25] C. Roth, N. Martz, F. Hahn, J.-M. Leger, C. Lamy, H. Fuess, J. Electr. Soc. 149 (2002) E433–E439.
[26] J.T. Richardson, Principles of Catalyst Development, Plenum Press, New York and London, 1989, pp. 23–82.
[27] G. Ertl, H. Knozinger, J. Weitkamp (Eds.), Handbook of Heterogeneous Catalysis, vol. 2, VCH, Weinheim, Federal Republic of Germany, 1997, pp. 752–767.
[28] C.A. Bessel, K. Laubernds, N.M. Rodriguez, R.T.K. Baker, J. Phys. Chem. B 105 (2001) 1115–1118.